Results in Physics 9 (2018) 815–818

Contents lists available at ScienceDirect

Results in Physics

journal homepage: www.elsevier.com/locate/rinp

On-chip remote charger model using plasmonic island circuit

J. Ali[a], P. Youplao[b], N. Pornsuwancharoen[b], M.S. Aziz[a], S. Chiangga[c], I.S. Amiri[d], S. Punthawanunt[e], G. Singh[f], P. Yupapin[g,h,*]

[a] Laser Centre, IBNU SINA ISIR, Universiti Teknologi Malaysia, 81310 Johor Bahru, Malaysia
[b] Department of Electrical Engineering, Faculty of Industry and Technology, Rajamangala University of Technology Isan, Sakon Nakhon Campus, 199 Phungkon, Sakon Nakhon 47160, Thailand
[c] Department of Physics, Faculty of Science, Kasetsart University, Bangkok 10900, Thailand
[d] Division of Materials Science and Engineering, Boston University, Boston, MA 02215, USA
[e] Multidisciplinary Research Center, Faculty of Science and Technology, Kasem Bundit University, Bangkok 10250, Thailand
[f] Department of Electronics and Communication Engineering, Malaviya National Institute of Technology Jaipur, 302017, India
[g] Computational Optics Research Group, Advanced Institute of Materials Science, Ton Duc Thang University, District 7, Ho Chi Minh City, Viet Nam
[h] Faculty of Electrical & Electronics Engineering, Ton Duc Thang University, District 7, Ho Chi Minh City, Viet Nam

ABSTRACT

We propose the remote charger model using the light fidelity (LiFi) transmission and integrate microring resonator circuit. It consists of the stacked layers of silicon-graphene-gold materials known as a plasmonic island placed at the center of the modified add-drop filter. The input light power from the remote LiFi can enter into the island via a silicon waveguide. The optimized input power is obtained by the coupled micro-lens on the silicon surface. The induced electron mobility generated in the gold layer by the interfacing layer between silicon-graphene. This is the reversed interaction of the whispering gallery mode light power of the microring system, in which the generated power is fed back into the microring circuit. The electron mobility is the required output and obtained at the device ports and characterized for the remote current source applications. The obtained calculation results have shown that the output current of $\sim 2.5 \times 10^{-11}\,AW^{-1}$, with the gold height of 1.0 μm and the input power of 5.0 W is obtained at the output port, which is shown the potential application for a short range free pace remote charger.

Whispering gallery mode (WGM) of light generated by the small-scale devices has been widely investigated and used [1–5]. One of them is the WGM generated by the microring resonator [6,7], which show the potential for the light source, energy source, and sensor application. The advantage of such a phenomenon is that the power of the propagation waves can generate within the system during the propagation without any connected port, which is convenient for some applications that the applied port is not allowed. Recently, Pornsuwancharoen et al. have shown the very promising work on the current source generated by the plasmonic island, where the light energy generated by the WGM can be converted to be the electrical energy by the stacked layer of silicon-graphene-gold layers. In this article, we are proposing the use the WGM generated by the microring resonator for the remote charger, especially, for the light fidelity (LiFi) transmission network use. Unfortunately, up to date there are not many works of the remote charger successfully employed [8–12]. In this work, the on-chip charger circuit is proposed. The mathematical model is formed by the reversed system of the WGM generation that is generated by the nonlinear microring resonator. The required electron mobility or electrical current is generated by the plasmonic island, where the light and electron energy can be exchanged via the plasmonic waves within the island layers. The simulation results are obtained and interpreted for the use of the LiFi charger application.

Light from the monochromatic light source is input into the system as shown in Fig. 1, the whispering gallery mode output is the electrical field output (E_{PI}), which is given by [6,7]

$$E_{PI}(\rho,\varphi) = \frac{4\pi\ cosech\left(k_{0n}\frac{\pi a}{2}\right)}{a^2 J_1^2(k_{0n}a)}\left[\frac{x_1\sqrt{k_1}}{\sqrt{1-2x_1y_1\cos(k_nL)+x_1^2y_1^2e^{-\alpha L}}}\right] \times \frac{(wA_0)\sqrt{k_0n_0}}{B^{\frac{1}{4}}}J_0(k_{0n}\rho)\int_0^a J_0(k_{0n}\rho)\left[\rho - \left(\frac{A}{2(B+C\rho^2)}+\frac{C}{4B}\right)\rho^3\right]d\rho \quad (1)$$

Eq. (1) is the electrical field in the cylindrical coordinate, where

* Corresponding author at: Computational Optics Research Group, Advanced Institute of Materials Science, Ton Duc Thang University, District 7, Ho Chi Minh City, Viet Nam.
E-mail address: preecha.yupapin@tdt.edu.vn (P. Yupapin).

https://doi.org/10.1016/j.rinp.2018.03.048
Received 11 January 2018; Received in revised form 14 February 2018; Accepted 22 March 2018
Available online 29 March 2018

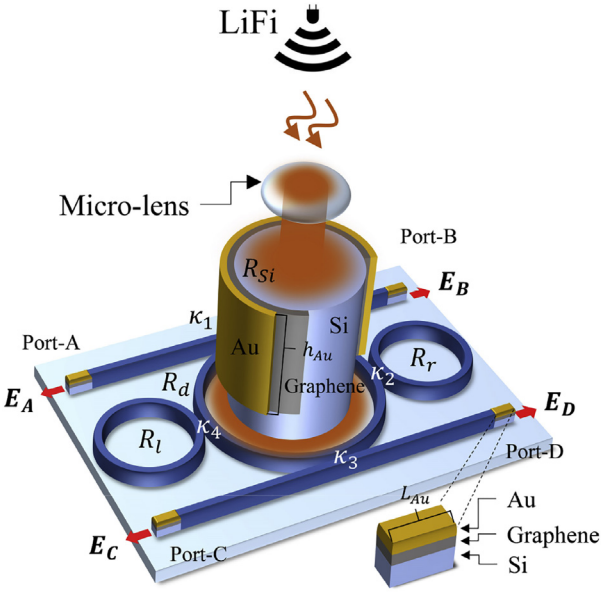

Fig. 1. A schematic of a LiFi charger, where R_d, R_r, l, are the ring radii of the center ring and two side rings, right (R_r) and left (R_l) hands, R_{Si}: Silicon ring radius. E_A, E_B, E_C, E_D are the electrical fields. The sensing and reference arms, input and drop ports are connected by the stacked silicon-graphene-gold layers, $\kappa_1 = \kappa_2 = \kappa_3 = \kappa_4 = 0.5$.

$A = k_{mn}^2 k_0^2 W^2 n_0^2 \rho^2$, $B = W^4 k_0^2 n_0^2$, $C = \varphi^2$, w, A_0 is constant of input signal. a is the radius of center ring, $x_1 = \sqrt{1-\gamma_1}$, $y_1 = \sqrt{1-\kappa_1}$, n_0 = linear refractive index. $k_0 = \frac{2\pi}{\lambda_0} n_{eff}$, n_{eff} is effective index, λ_0 is input wavelength, ρ and φ are the cylindrical coordinate radius and phase, respectively. κ_1, γ_1 is the coupling constant and attenuation coefficient between linear waveguide and center of Panda ring resonator, respectively. k_{0n} is the wave number in the Bessel's function (J_0) by n is mode of electromagnetic field, and L is the center ring circumference.

In Fig. 1, the resonant output is the reversed WGM output of the equation [1], which is the driven group velocity and mobility in terms of optical and electrical aspects. The relationship between the light intensity (I), group velocity and the electron mobility can be expressed as $I = E^2 = \left(\frac{V_d}{\mu}\right)^2$, which is defined by $V_d = \mu E$. When an electric field E is applied to the grating sensor, an electric current is established in the conductor. The density J_s of this current is given by $J_s = \sigma E$. The constant of proportionality σ is called the specific conductance or electrical conductivity of the conductor (gold is $1.6 \times 10^8\,\mathrm{W^{-1}\,m^{-1}}$) [13–17].

The advantage of the modified add-drop filter with two side rings is that the nonlinear effect can offer the shorter output pulse width and easier WGM resonant output control than the original system. The electron mobility in a gold material is $42.6\,\mathrm{cm^2\,V^{-1}\,s^{-1}}$, the electron mass is 9.10×10^{-31} kg, the electron charge is 1.60×10^{-19} C. The refractive index of the silicon is 1.46. The linear and nonlinear refractive indices of the GaAsInP/P are 3.14 and $1.30 \times 10^{-13}\,\mathrm{m^2\,W^{-1}}$, respectively. The attenuation coefficient of the waveguide is $0.1\,\mathrm{dB\,(mm)^{-1}}$. In a simulation, the input power from the remote source is entered into the island via the coupling lens. The input power was varied from 0.5 to 5.0 W, the different gold layer heights were varied from 200 to 1000 nm. The simulation results are as shown in Figs. 2 and 3. The plot of the relationship between the input power and the mobility output for all circuit output ports is shown in Fig. 2, which is shown the very interesting result. In Fig. 3 shows the result of the current outputs at the different output ports and the island.

The output mobility within the plasmonic island is driven by the group velocity generated by the WGM within the modified add-drop filter, which can be changed to be the output current. The relationship between the light intensity (I), group velocity and the electron mobility can be expressed as $I = E^2 = \left(\frac{V_d}{\mu}\right)^2$, which is defined by $V_d = \mu E$. When an electric field E is applied to the grating sensor, an electric current is established in the conductor. The density J_s of this current is given by $J_s = \sigma E$. The required current output is given by the results in Fig. 3(c), where the linear relationship between the input power and the output current is obtained. The various gold heights can be selected for each specific purpose. The low current (mobility) can be driven by the input light via the gold layer at the input port, from which the output current can be amplified and used as the current source for the charger. The relationship between the input power and the output current is shown in Fig. 3(c), while the geometry size has been given by the figure caption in Fig. 2, which was also described by the authors in reference [16,17].

We have shown that the light fidelity network has become the promising system that can accommodate the large capacity demands. Because it can offer the large bandwidth (high bit rate). Apart from that, the free space transmission can provide the light power that can be used for other purposes, for an instant, for a remote area charger. In this article, we have modelled the LiFi charger using the plasmonic island embedded within the microring resonator. By using the selected parameters obtained from the graphical method called the "Optiwave" program, the obtained simulation has shown the very interesting results, in which the current output of the output mobility and current of $\sim 1.0 \times 10^{-10}\,\mathrm{cm^2\,V^{-1}\,s^{-1}\,W^{-1}}$ and $\sim 2.5 \times 10^{-11}\,\mathrm{AW^{-1}}$ are obtained, with the gold height and the input power of 1.0 μm and 5 W, respectively.

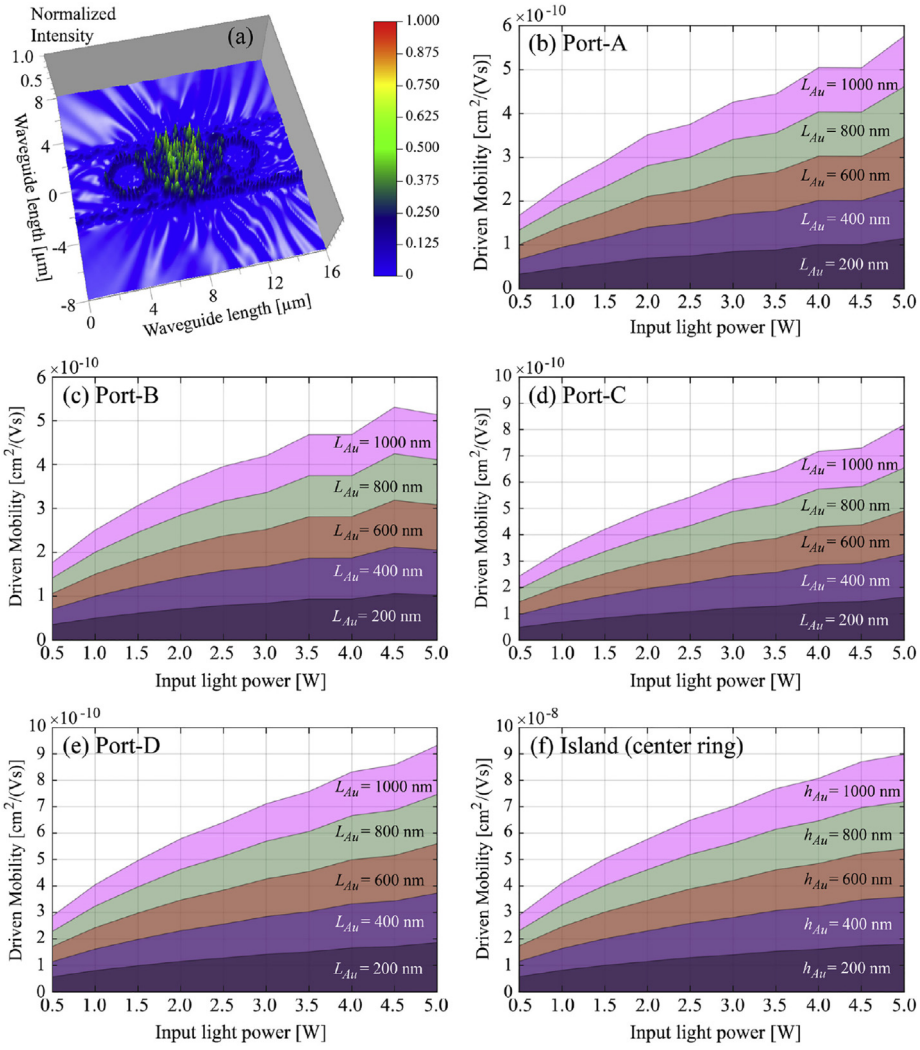

Fig. 2. The results; (a) the 3D Opti-wave result of the system in Fig. 1 for preliminary investigation, the parameters are the input power = 1.0 W, R_d = 2.1 μm, R_l = R_r = 1.4 μm, R_{Si} = 1.55 μm; and (b)–(f) are the plots of the mobility outputs, where the data is obtained by simulation using the MATLAB program. The gold layer parameters are w = 0.5 μm, thickness = 0.5 μm, the gold island parameters are thickness = 0.5 μm, the practical R_{Si} is added up by graphene of 0.5 μm and gold of 0.5 μm.

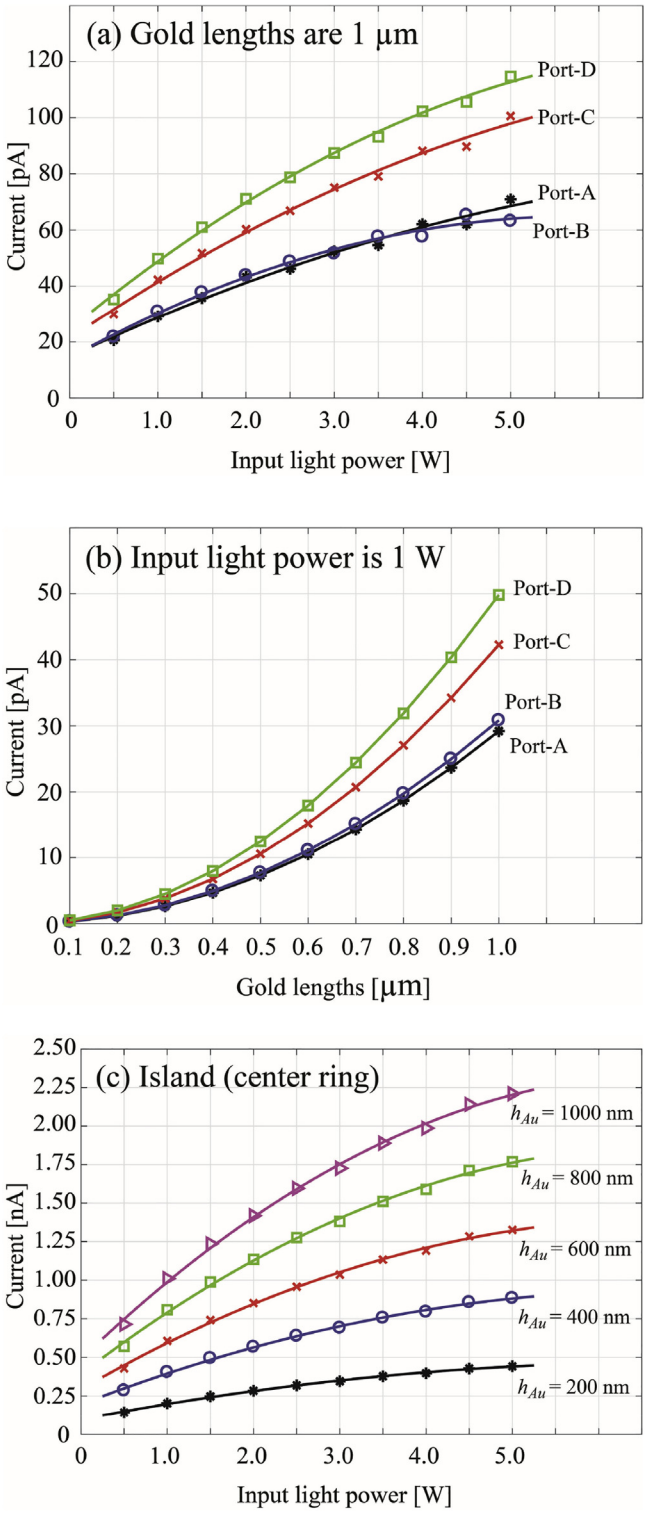

Fig. 3. The plots of the mobility outputs, where the data is obtained by simulation using the MATLAB program. The solid line is the fitting curve, the output current are (a) fixed the gold length at 1 μm, (b) fixed the input light power at 1 W, and (c) gold height and input power variations.

Acknowledgment

The authors would like to give the appreciation for the research financial support and the research facilities from the Universiti Teknologi Malaysia, Johor Bahru, Malaysia.

Appendix A. Supplementary data

Supplementary data associated with this article can be found, in the online version, at http://dx.doi.org/10.1016/j.rinp.2018.03.048.

References

[1] He L, Ozdemir SK, Zhu J, Kim W, Yang L. Detection single viruses and nanoparticles using whispering gallery microlasers. Nat Nanotechnol 2011;6:428–32.
[2] Foreman MR, Swaim JD, Vollmer F. Whispering gallery mode sensors. Adv Opt Photon 2015;7:632–8.
[3] Zhang C, Cocking A, Freeman E, Lui Z, Tadigadapa S. On-chip glass microspherical shell whispering gallery mode resonators. Sci Rep 2017;7:14965.
[4] Vollmer F, Arnold S. Whispering-gallery-mode biosensing: label-free detection down to single molecules. Nat Methods 2008;5:591–6.
[5] Foreman MR, Swaim JD, Vollmer F. Whispering gallery mode sensors. Adv Opt Photon 2015;7:168–240.
[6] Pornsuwancharoen N, Youplao P, Amiri IS, Ali J, Yupapin P. Electron driven mobility model by light on the stacked metal-dielectric-interfaces. Microw Opt Technol Lett 2017;59(7):1704–10.
[7] Phatharacorn P, Chiangga S, Yupapin P. Analytical and simulation results of a triple micro whispering gallery mode probe system for a 3D blood flow rate sensor. Appl Opt 2016;55(33):9504–13.
[8] Zhang J, Song G, Li Y, Qiao G, Li Z. Battery swapping and wireless charging for a home robot system with remote munan assistance. IEEE Trans Consum Electron 2013;59(4):747–55.
[9] Thangavelu A, Vairakannu S, Pavathyshankar D. Linear open circuit voltage-variable step-size-incremental conductance strategy-based hybrid MPPT controller for remote power applications. IET Power Electron 2017;10(1):1363–76.
[10] Chen J, Li S, Chen S, He S, Shi S. Q-charge: a quadcopter-based wireless charging platform for large-scale sensing applications. IEEE Network 2017;31(6):56–61.
[11] Assawaworrarit S, Yu X, Fan S. Robust wireless power transfer using a nonlinear parity–time-symmetric circuit. Nature 2017;546:354–5.
[12] Nuwer R. Wireless charging with sound waves. Sci Am 2014;311:52–7.
[13] Thomas PA, Auton GH, Kundys D, Grigorenko AN, Kravets VG. Strong coupling of diffraction coupled plasmons and optical waveguide modes in gold stripe dielectric Nano-structures at telecom wavelengths. Sci Rep 2017;7:45196.
[14] Gall D. Electron mean free path in elemental metals. J Appl Phys 2016;119:085101.
[15] Baccarani G, Ostoja P. Electron mobility empirically related to the phosphorus concentration in silicon. Solid State Electron 1975;18(6):579–80.
[16] Ali J, Pornsuwancharoen N, Youplao P, Aziz MS, Chiangga S, Jaglan J, Amiri IS, Yupapin P. A novel plasmonic interferometry and the potential applications. Results Phys 2018;8:438.
[17] Pornsuwancharoen N, Amiri IS, Suhailin FH, Aziz MS, Ali J, Singh G, Yupapin P. Micro-current source generated by a WGM of light within a stacked silicon-graphene-Au waveguide. IEEE Photon Technol Lett 2017;19:1768–71.